Surface electronic structure of heavily-ion-implanted and laser-annealed Si single crystals

Fulvio Parmigiani*
Centro Informazioni Studi Esperienze, S.p.A., Casella Postale 12081, I-20134 Milano, Italy

Paul S. Bagus and Gianfranco Pacchioni
IBM Research Division, Almaden Research Center, San Jose, California 95120-6099

Angiolino Stella
Dipartimento di Fisica "Alessandro Volta," Università degli Studi di Pavia, via Bassi 6, I-27100 Pavia, Italy
(Received 11 August 1989)

This paper presents angle-resolved photoemission spectroscopy data of the core lines of a heavily implanted and laser-annealed Si(100) surface. For the first time unambiguous data show that the laser-annealing process induces an almost complete reconstruction of the inner-layer electronic structure, whereas the outermost layers preserve the behavior of the ion-implanted surface. *Ab initio* electronic structure calculations performed on a Si_nH_{3n-3} cluster strongly indicate that the modifications observed are due to the loss of coordination of the Si atoms, which is recovered after laser annealing only in the inner layers.

I. INTRODUCTION

Ion implantation requires a subsequent thermal treatment to remove the damage and to electrically activate the implanted dopant atoms. Several procedures have been used: heat treatment in a furnace for a time interval of hours, rapid thermal annealing for a time interval of a few seconds, and pulsed-laser irradiation in a time interval ranging from nanoseconds to picoseconds. The structure of the ion-implanted layer after annealing has been investigated by several analytical techniques.[1-10] In many cases the information shows the residual damage and the overall electrical characteristics of the doped layer. The electrical properties are related to the spatial arrangements of the silicon atoms in the very last surface layers. This region is not as easy to investigate by the usual techniques and it should depend on the annealing procedure adopted.

The surface electronic structure of a (heavily) ion-implanted and subsequently annealed Si single crystal is still rather poorly understood.[4] This is especially true, for instance, with respect to the knowledge of the mechanisms of reconstruction induced by the rapid process of melting and solidification on the outermost surface region, $\simeq 20$ Å thick.

The importance of an unambiguous understanding of the surface structure of a heavily ion-implanted and annealed semiconductor arises both from technological and scientific considerations.[10] As device dimensions become increasingly smaller, the near-surface region will become even more important, and it will be necessary to pay more attention to the knowledge of its electronic and crystallographic structure. On the other hand, in the case of pulsed irradiation a knowledge of the surface electronic structure may be useful for determining the driving mechanisms of the liquid-phase epitaxial regrowth that follows the melting due to the rapid deposition of energy from a Q-switched laser.

In this paper, we present angle-resolved photomission spectroscopy (ARPS) data, obtained on an As-implanted Si(100) single-crystal surface annealed by a Nd: glass (neodymium-doped yttrium iron garnet) pulsed laser. The data show that the laser-annealing process induces almost a complete reconstruction of the inner layer's structure, whereas the outermost layer is still disordered, and it shows the same behavior as the ion-implanted surface. *Ab initio* electronic structure calculations performed on a Si_nH_{3n-3} cluster are used to interpret the experimental data. This model strongly indicates that the modifications observed in the Si $2p$ electronic structure of the ion-implanted surface are due to the loss of coordination of the Si atoms. The correct coordination is recovered after laser annealing in the inner layers, whereas the outermost layers keep their lattice disoder.

II. EXPERIMENTAL

$\langle 100 \rangle$ silicon-oriented silicon wafers were implanted with 100-keV As^+ at a current of $\simeq -2$ mA and an average current density of $\simeq 10\ \mu A\,cm^{-2}$. The electron beam electrostatically scanned on an optically polished 4-in.-diameter wafer about 500 μm thick. In the specific case considered here a fluence of 10^{15} As^+ cm^{-2} was adopted. Annealing of the implanted layers was performed with neodymium-glass-pulsed laser of 30-nsec duration and an energy density of up to 2 $J\,cm^{-2}$. The As profiles as well as the quality of the surface region were determined by 2-MeV He^+ backscattering in combination with channeling. No evidence of As atoms was found on the surface. Before transferring the samples into the ultrahigh-vacuum (UHV) analysis apparatus, surface contaminants were eliminated by etching the sample surface using a 50% dilute HF acid in an inert at-

mosphere.[8] The etching time and the acid concentration were sufficient to remove only the possible SiO_x present on the Si surface. After the etching, the samples were directly transferred through an UHV interlock into the analysis chamber of an ARPS monochromatized system, a Perkin-Elmer 5300. The total contaminants, i.e., C, O, and F, concentration was less than $\frac{1}{10}$ of a monolayer when survey spectra were taken at a takeoff angle of 20°.

III. RESULTS

The calibration of the spectrometer was performed using the Si(100) surface of a single crystal which was cleaned using the method described above. The ultimate resolution of the instrument, as measured on the Si $2p$ core lines using a pass energy of 4.5 eV, was 0.35 eV. Figure 1(a) shows the Si $2p$ cores lines as measured in this experiment; in Table 1(a) the Si $2p$ core-line experimental

TABLE I. (a) XPS deconvolution data of the Si(100) single crystal and As-ion-implanted surface measured at takeoff angles of 10°, 45°, 60°, and 90°. The data marked by asterisks refer to Si $2p$ core lines of the threefold- and twofold-coordinated Si atoms. The core-line intensities $I2p$ have been measured from the respective XPS line areas. (b) XPS deconvolution data of the laser-annealed Si(100) As-ion-implanted surface as measured at 10°, 25°, 45°, 60°, and 90°. Symbol captions are given in Table I(a).

Sample	Takeoff angles	Si core lines	Binding energy (eV)	FWHM (eV)	$(\Delta\varepsilon)_{2p_{3/2}-2p_{3/2*}}$ (eV)	Core-line ratio $\frac{I_{2p_{3/2}}}{I_{2p_{1/2}}}$	Core-line ratio $\frac{I_{2p_{3/2}}}{I_{2p_{3/2*}}}$
				(a)			
	45°	$2p_{3/2}$	99.0	0.39		2.0	
		$2p_{1/2}$	99.6	0.42			
Si(100) ion impl.	10°	$2p_{3/2}$	99.06	0.45	0.38	2.0	0.64
		$2p_{1/2}$	99.68	0.45			
		$2p_{3/2*}$	99.44	0.60			
		$2p_{1/2*}$	100.05	0.60			
Si(100) ion impl.	45°	$2p_{3/2}$	99.06	0.45	0.29	1.97	0.44
		$2p_{1/2}$	99.68	0.45			
		$2p_{3/2*}$	99.35	0.45			
		$2p_{1/2*}$	99.95	0.57			
Si(100) ion impl.	60°	$2p_{3/2}$	99.04	0.48	0.30	2.0	0.76
		$2p_{1/2}$	99.66	0.48			
		$2p_{3/2*}$	99.34	0.54			
		$2p_{1/2*}$	99.95	0.54			
Si(100) ion impl.	90°	$2p_{3/2}$	99.06	0.46	0.29	1.92	0.80
		$2p_{1/2}$	99.68	0.45			
		$2p_{3/2*}$	99.35	0.54			
		$2p_{1/2*}$	99.95	0.54			
				(b)			
	10°	$2p_{3/2}$	99.06	0.54	0.36	1.9	1.06
		$2p_{1/2}$	99.68	0.54			
		$2p_{3/2*}$	99.42	0.62			
		$2p_{1/2*}$	100.02	0.62			
	25°	$2p_{3/2}$	99.10	0.46	0.32	1.84	1.04
		$2p_{1/2}$	99.71	0.46			
		$2p_{3/2*}$	99.42	0.58			
		$2p_{1/2*}$	100.04	0.62			
	45°	$2p_{3/2}$	99.10	0.46	0.32	2.0	1.35
		$2p_{1/2}$	99.71	0.46			
		$2p_{3/2*}$	99.42	0.58			
		$2p_{1/2*}$	100.04	0.62			
	60°	$2p_{3/2}$	99.05	0.41	0.35	2.0	1.55
		$2p_{1/2}$	99.70	0.43			
		$2p_{3/2*}$	99.40	0.60			
		$2p_{1/2*}$	100.01	0.62			
	90°	$2p_{3/2}$	99.06	0.41	0.38	1.99	1.84
		$2p_{1/2}$	99.69	0.43			
		$2p_{3/2}$	99.44	0.62			
		$2p_{1/2*}$	100.06	0.62			

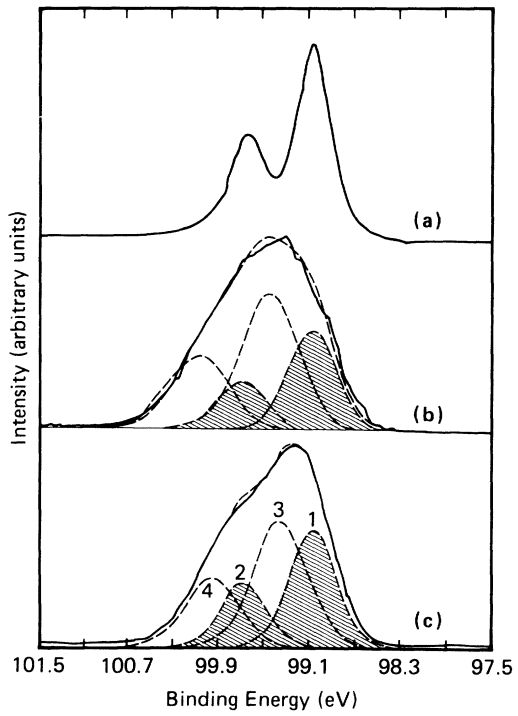

FIG. 1. Si $2p$ XPS spectrum of the Si(100) surface measured by a takeoff angle of 45° (a). Si $2p$ XPS spectrum of the Si(100) surface of a heavily As-ion-implanted Si single crystal wafer measured at a takeoff angle of 10° (b) and 90° (c). The parameters of the ion implantation are reported in the text.

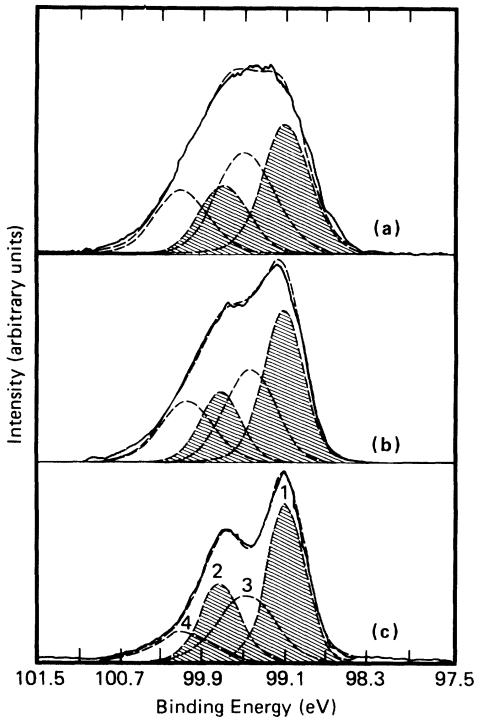

FIG. 2. Si $2p$ XPS spectra of a heavily As-ion-implanted ⟨100⟩ silicon wafer after laser annealing measured at 10° (a), 45° (b), and 90° (c). The laser annealing parameters are reported in the text.

parameters are reported. Figures 1(b) and 1(c) show the Si $2p$ spectra of the Si(100) (As^+) ion-implanted surface as measured at takeoff angles of 10° and 90°, respectively. A significant change is noticed when curve 1(a) is compared with curves 1(b) and 1(c). Since it has been demonstrated that the loss of coordination could induce an upward shift of $\simeq 1$ eV on the core orbital binding energies,[11] the broadening of the Si $2p$ lines observed on Si-ion-implanted samples could be attributed to the loss of coordination of some Si atoms. In this framework, the deconvolution reported in Figs. 1(b) and 1(c) have been performed assuming for the line 1 and 2 the spectral parameters of the Si $2p_{3/2}$ and Si $2p_{1/2}$, respectively, as measured on a well-ordered Si(100) surface, while the spectral parameters for the peaks 3 and 4 have been chosen in order to fit the experimental curves. Table I gives the parameters of the deconvolution for XPS measurements performed at 10°, 25°, 45°, 60°, and 90°. Figures 1 and 2 and Tables I(a) and I(b) show that the binding-energy difference $\Delta\varepsilon$ between peaks 1 and 3 is $\simeq 0.30$ eV. This parameter can be compared with theoretical data obtained from *ab initio* electronic structure calculations performed on Si atoms with different coordination (fourfold versus threefold and twofold coordination).

It should be noted that, on the basis of this interpretation, the intensity ratio between peaks 1 and 3 is related to the degree of the induced crystal disorder.

Figures 2(a) and 2(c) show the Si $2p$ core lines of a laser-annealed area as measured at takeoff angles of 10°, 45°, and 90°. The differences between the spectra for the annealed and unannealed cases are significant. Using the same deconvolution parameters obtained for the unannealed surface, Figs. 1(a) and 1(c), it is clear that the laser-annealing effects are different in the topmost layers than in the deeper layers. For the Al $K\alpha$ line and a takeoff angle of 10°, the sampled depth is $\simeq 5$ Å, with a takeoff angle of 90°, it is $\simeq 30$ Å, thus it is possible to infer that there exists a gradient of the crystal reconstruction between the surface and the first 30 Å; Table I(b) summarizes this data.

IV. THEORY AND DISCUSSION

In order to verify this interpretation of the x-ray photoemission spectroscopy (XPS) $2p$ binding-energy (BE) shifts as arising from the coordination of the ionized Si atom, we have obtained *ab initio* theoretical core-level BE's for cluster models which contain differently coordinated Si atoms. The three clusters, Si_3H_6, Si_4H_9, and Si_5H_{12}, which contain twofold-, threefold-, and fourfold-coordinated Si atoms, respectively, are shown in Fig. 3. The central Si atom of each cluster has two, three, or four Si near neighbors at the bulk crystal Si-Si distance of 2.4 Å. These neighboring Si atoms are each surrounded by 3 H atoms which force the bulk sp^3 hybridization and simulate the reminder of the crystal; see Ref. 11. Self-consistent field (SCF) wave functions have been computed for these clusters following the general approach in Ref. 11. The ground state of T_d symmetry Si_5H_{12} is a closed-

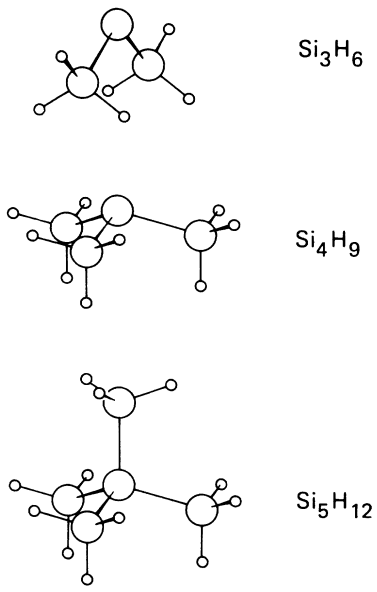

FIG. 3. Geometry of the Si_3H_6, Si_4H_9, and $Si_5H_{(12)}$ clusters used to model twofold-, threefold-, and fourfold-coordinated Si atoms. The Si-Si distance has been fixed to the bulk value, i.e., $d_{(Si\text{-}Si)}=4.44$ bohrs. The Si-H distance is that of SiH_4, i.e., $d_{(Si\text{-}H)}=2.80$ bohrs.

shell singlet, while the wave functions for $C_{3v}Si_4H_9$ and $C_{2v}Si_3H_6$ are open shell and contain Si dangling bonds. For Si_3H_6, the two Si dangling bonds have been coupled high spin to give a triplet state. Large LCAO (linear combination of atomic orbitals) basis sets have been used for the Si atom in order to reduce the basis-set superposition error (BSSE) for the central Si atom. This error arises because the basis sets on the neighboring Si atoms are used to improve the description of the atomic character of the central Si atom.[12] Clearly, the BSSE is a coordination-dependent error and will give misleading, nonphysical, results for the BE shifts for differently coordinated atoms. As well as using a large Si basis set, we have also calculated the BE shifts with a procedure which takes into account the remaining small BSSE (see below).

We consider the core-level BE shifts for differently coordinated Si using the Koopman's theorem (KT) initial-state cluster ionization potentials (IP's) for ionization of the central atom in each cluster. The KT IP is simply taken as the orbital energy $-\varepsilon_i$ of the shell from which the electron is removed. This is the initial state IP for closed-shell Si_5H_{12}; for open-shell Si_3H_6 and Si_4H_9, it is the IP to the weighted average of the different multiplets formed when a core level is ionized.[13] These multiplets will give a broadening for the core-level XPS peaks of the twofold- and threefold-coordinated Si atoms which have open-shell dangling bonds. This broadening is observed in the peaks labeled 2 and 4 in Figs. 1 and 2 for the ion-implanted Si $2p$ XPS spectra and is consistent with our assignment of these peaks to ionization of Si atoms with twofold or threefold coordination. Finally, we note that the cluster point group symmetry splits the $2p_x$, $2p_y$, and $2p_z$ levels for the twofold- and threefold-coordinated atoms; in the following, we use the average energy of these levels. The KT IP's are significantly larger than observed core-level IP's because Koopman's theorem neglects the final-state relaxation. However, there is good reason to believe that the relaxation energy will be similar for differently coordinated atoms[14] and that the initial-state KT IP shifts for these atoms will accurately reflect the observed XPS BE shifts. We have computed the shifts of the core-level KT IP's of the central Si atom in a way which eliminates any errors due to basis-set superposition effects. The self-consistent-field (SCF) wave function for the free Si atomic ^3P wave function is computed using the basis sets for the Si atom *but* also including the basis sets for the surrounding Si and H atoms which would be present in a Si_nH_m cluster. This atomic wave function is described as using "ghost" basis sets and the orbital energies are denoted $\varepsilon_i(\text{Si};\text{Si}_n\text{H}_m$ ghost); a different "ghost" basis set is used to obtain a Si-atom description appropriate for comparison with each cluster. The shift of the KT IP of a core level of an n-fold-coordinated Si atom with respect to the free Si atom is denoted $\Delta\varepsilon_i$ (n-fold coordinated) and is given by

$$\Delta\varepsilon_i(n\text{-fold-coordinated}) = -[\varepsilon_i(\text{Si};\ \text{Si}_n\text{H}_m\ \text{ghost}) - \varepsilon_i(\text{Si}_n\text{H}_m)] \ . \quad (1)$$

For the large basis set which we have used for Si, Eq. (1) gives KT IP shifts very close to those which would be obtained with infinitely large basis sets.

For the Si $1s$, $2s$, and $2p$ core levels, the $\Delta\varepsilon_i$ shifts of Eq. (1) are to lower binding energy for atoms with higher coordination. For metals, this shift has been related to the increase in the electron charge density which surrounds atoms with higher coordination.[14] We give in Table II the $\Delta\varepsilon_i$ KT shifts renormalized to the IP for a fourfold-coordinated Si taken as zero. The shifts now appear as shifts to *larger* BE for atoms with *lower* coordination than bulk Si. This shift is larger for the $1s$ core levels than for the $2s$ and $2p$ semicore levels. For the $2p$ BE, the shifts for twofold- and threefold-coordinated Si are similar, and they are $\simeq 0.3$ eV. This computed BE shift due to the lowering of the Si coordination is reasonably close to the XPS shifts measured for the $2p_{3/2}$ levels for ion-implanted Si(100) surfaces, as reported in Tables I(a) and I(b). This agreement gives strong evidence for the origin of these observed shifts as a coordination effect.

TABLE II. Core-level binding-energy shifts in (eV) with respect to the fourfold-coordinated Si.

	$\Delta\varepsilon$ ($1s$)	$\Delta\varepsilon$ ($2s$)	$\Delta\varepsilon$ ($2p$)
Coordination 4 (Si_5H_{12})	0.0	0.0	0.0
Coordination 3 (Si_4H_9)	0.28	0.20	0.27
Coordination 2 (Si_3H_6)	0.39	0.23	0.30

V. CONCLUSIONS

In conclusion, ARPS applied to a heavily ion-implanted and laser-annealed Si surface gives new and important information on the local order near the topmost layers. In laser-annealed (100) Si, a comparison between the curves taken at takeoff angles of 10° and 90° is coupled with model calculations concerning the dependence of the core-level binding energies on the coordination of the Si atoms. This presents for the first time clear evidence of a gradient in the crystalline order, where such a behavior was not expected or sufficiently known.

ACKNOWLEDGMENTS

The authors wish to thank Dr. H. Goretzki and Dr. U. Roll of the Perkin Elmer Labortorier, Vatterstetten, F.R.G., for their cooperation on the XPS measurements. Professor E. Rimini and Professor Campisano of the University of Catania (Italy) are also acknowledged for supplying the samples and for the helpful discussions.

---

*Present address: IBM Research Division, Almaden Research Center (K31/802), 650 Harry Road, San Jose, CA 95120-6099.

[1] *Ion Implantation: Science and Technology,* edited by J. F. Ziegler (Academic, New York, 1984).

[2] C. W. White, D. M. Zehner, S. U. Campisano, and G. A. Cullis, in *Surface Modification and Alloying,* edited by J. M. Poate, G. Foti, and D. C. Jacobson (Plenum, New York, 1983).

[3] D. G. Beanland, in *Ion Implantation and Beam Processing,* edited by J. E. Williams and J. M. Poate (Academic, New York, 1984), Chap. 8, p. 262.

[4] M. Servidori, S. Cannavo, G. Ferla, A. La Ferla, and E. Rimini, Appl. Phys. A **44**, 213 (1987).

[5] U. Campisano, E. Rimini, A. Borghesi, G. Guizzetti, L. Nosenzo, and A. Stella, Phys. Scr. **19B**, 544 (1987).

[6] H. Engstrom, J. Appl. Phys. **51**, 245 (1980).

[7] D. E. Aspnes, S. M. Kelso, C. G. Olson, and D. W. Lynch, Phys. Rev. Lett. **48**, 1863 (1982).

[8] D. E. Aspnes, M. Erman, J. B. Theeten, P. Chambon, and S. M. Kelso, J. Appl. Phys. **56**, 2664 (1984).

[9] P. D. Paray, J. Vac. Sci. Technol. **58**, 2773 (1985).

[10] A. Borghesi, Chen Chen-Jia, G. Guizzetti, L. Nosenzo, A. Stella, E. Rimini, and U. Campisano, J. Appl. Phys. **58**, 2773 (1985).

[11] M. Seel and P. S. Bagus, Phys. Rev. B **20**, 1603 (1979).

[12] P. S. Bagus, K. Hermann, and C. W. Bauschlicher, J. Chem. Phys. **80**, 4378 (1984).

[13] K. Herman and P. S. Bagus, Phys. Rev. B **16**, 4195 (1977).

[14] C. J. Nelin and P. S. Bagus, in *Festkörperprobleme,* edited by P. Grosso (Vieweg, Braunschweig, 1985), Vol. XXV, p. 135; P. S. Bagus, in *Elemental and Molecular Clusters,* edited by G. Benedek, P. Martin, and G. Pacchioni (Springer, Heidelberg, 1988), p. 286.